

A11102 128985

NAT'L INST OF STANDARDS & TECH R.I.C.



A11102128985

/Bureau of Standards Journal of research  
QC1 .U52 V8:1932 C.1 NBS-PUB-C 1928



# GRAPHICAL DETERMINATION OF POLAR PATTERNS OF DIRECTIONAL ANTENNA SYSTEMS

By G. L. Davies and W. H. Orton

## ABSTRACT

This paper describes graphical methods for the determination of polar patterns of directional antenna systems. These methods are less tedious and more generally applicable than computation from available mathematical equations.

At any distant point, the relative phases of the disturbances from the individual antennas of an array are dependent upon the differences in the paths from the antennas to the point, and upon the relative phases of the antenna currents. The path differences may be readily constructed on a scale drawing of the array, and by means of a special protractor these path differences are converted to phase angles for the construction of a vector diagram representing the disturbances at the field point. The resultant of this vector diagram gives the field intensity at that point. Such diagrams for a number of points equidistant from the array give the relative field intensities in various directions and thus enable a polar pattern to be drawn.

As illustrations, the polar patterns of two very simple arrays are determined; a broadside array of two antennas spaced one-half wave length and carrying equal equiphased currents; and an end-on array of two antennas spaced one-quarter wave length and carrying equal currents in time quadrature.

By a principle for the addition of the directive patterns of groups of antennas, the work involved in determining patterns of arrays containing a large number of antennas may be greatly simplified. This method also permits ground effects to be readily included, the image current being calculated by means of equations given by Wilmette.

## CONTENTS

	Page
I. Introduction.....	555
II. General method.....	556
III. Applications of method.....	559
IV. Conclusion.....	569

## I. INTRODUCTION

During the course of a study of the characteristics of directional antenna systems, undertaken in connection with experimental work on the use of a high-frequency beam as an aid in the blind landing of aircraft, it was found that existing mathematical methods for plotting the polar patterns of antenna arrays were in many cases quite tedious. Furthermore, most of the equations now available apply only to somewhat restricted classes of arrays, so that, in order to plot the directional pattern of an array not included in such classes, it was necessary first to develop the equation of the pattern. A definite need was felt for a rapid and less tedious method of determining these diagrams. The graphical methods<sup>1</sup> presented here were found to save much time and labor and to be quite general in their application to what may be termed planar arrays; that is, arrays whose individual antennas are so arranged that their midpoints lie in the same plane.

The mathematical equations available for the computation of directional diagrams have been developed by numerous investigators,

<sup>1</sup> A graphical treatment from a somewhat different viewpoint appeared in Marconi Review No. 33, pp. 11-18, November-December, 1931, while the present paper was in press.



notably Foster,<sup>2</sup> Fleming,<sup>3</sup> Green,<sup>4</sup> Wilmotte,<sup>5</sup> and Southworth.<sup>6</sup> Wells<sup>7</sup> has given a graphical method based on Green's analysis. This method, however, is subject to important limitations which, although not mentioned by Wells, are evident from the analysis given by Green.

## II. GENERAL METHOD

All methods for the determination of polar patterns of antenna arrays involve the calculation of the vector sum of the effects, at a distant point, due to the individual antennas or elements of the array. For simplicity, the present discussion is limited to planar arrays in which the elements are parallel and one-half wave length long.

The radiation from an isolated half-wave antenna, in a plane perpendicular to the antenna, is equal in all directions; that is, the polar pattern is a circle. In a plane containing the antenna, the radiation is approximately represented by the polar pattern  $r = \cos \theta$ ,

the direction  $\theta = 0$  being perpendicular to the antenna. This pattern consists of two circles each tangent to the other and to the antenna.

For the purposes of analysis, the half-wave elements of a planar array may be considered equivalent to point sources located at their centers. The individ-

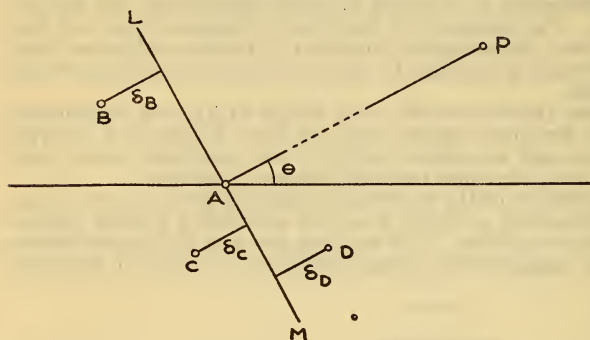


FIGURE 1.—A group of four point-sources and their respective retardations  $\delta$  in the direction of  $P$

ual directivity of these elements in their containing plane will be accounted for and discussed later.

In Figure 1, antennas are located at  $A, B, C, D$ , the currents in them being considered, for the moment, as equiphased. If  $P(r, \theta)$  is taken to be sufficiently distant, the lines joining it with  $A, B, C$ , and  $D$ , are sensibly parallel. Under this condition, periodic disturbances originating at any point on the line  $LM$  perpendicular to  $AP$  will be in phase at  $P$ . This phase is taken as a reference. Then a disturbance originating at a point, such as  $D$ , on the near side of  $LM$  will have a positive phase angle, while one originating at a point, such as  $B$  or  $C$ , on the far side of  $LM$  will have a negative phase angle. This phase angle, which will be denoted by  $\phi$  is equal to  $2\pi \frac{\delta}{\lambda}$ , where  $\lambda$  is the wave length and  $\delta$  is the path difference; that is, the distance from

<sup>2</sup> R. M. Foster, *Directive Diagrams of Antenna Arrays*, Bell System Tech. J., vol. 5, p. 292, April, 1926.

<sup>3</sup> J. A. Fleming, *Approximate Theory of the Flat Projector (Franklin) Aerial Used in the Marconi Beam System of Wireless Telegraphy*, Experimental Wireless, vol. 4, p. 387, July, 1927.

<sup>4</sup> E. Green, *Calculation of the Polar Curves of Extended Aerial Systems*, Experimental Wireless, vol. 4, p. 587, October, 1927.

<sup>5</sup> R. M. Wilmotte, *General Considerations of the Directivity of Beam Systems*, J. I. E. E., vol. 66, p. 955, September, 1928. *General Formulas for the Radiation Distribution of Antenna Systems*, J. I. E. E., vol. 68, p. 1174, September, 1930. *The Radiation Distribution of Antennae in Vertical Planes*, J. I. E. E., vol. 68, p. 1191, September, 1930.

<sup>6</sup> G. C. Southworth, *Certain Factors Affecting the Gain of Directive Antennas*, Proc. I. R. E., vol. 18, p. 1502, September, 1930. Bell System Tech. J., vol. 10, p. 63, January, 1931.

<sup>7</sup> N. Wells, *Beam Wireless Telegraphy*, Elect. Rev., vol. 102; Part I, p. 898, May 25, 1928; Part II, p. 940, June 1, 1928.

the line  $LM$  to the antenna. The phase angle of the disturbance from  $B$  is therefore  $\phi_B = -2\pi \frac{\delta^B}{\lambda}$ , that from  $C$  is  $\phi_C = -2\pi \frac{\delta^C}{\lambda}$ , and that from  $D$  is  $\phi_D = 2\pi \frac{\delta^D}{\lambda}$ . The sign of  $\delta$ , and, therefore, of  $\phi$  may be readily determined by the following rule: Consider  $\delta$  to be directed from the reference line  $LM$  (fig. 1) toward the antenna with which it is associated; then  $\delta$  (and thus  $\phi$ ) is positive when it points toward  $P$  and negative when it points away from  $P$ .

Since the antenna currents were assumed to be equiphased these phase angles  $\phi$  determine the directions of the rotating vectors representing the disturbances at  $P$  due to each antenna. The relative magnitudes of these vectors are determined by the amplitudes of the respective antenna currents. If an arbitrary length is chosen for one of the vectors (preferably the one representing the disturbance whose phase has been taken as reference), a vector diagram may be constructed whose resultant represents the electric field intensity at  $P$  due to the antenna array. If the antenna currents are not equiphased as assumed,

then the direction of the vector at  $P$  representing the disturbance due to an element will be  $\phi + \alpha$ , where  $\alpha$  is the phase angle of the current in that element with respect to the reference element and is positive for leading and negative for lagging phase angles.

This construction is shown in Figure 2. If such vector diagrams are drawn for a number of similar points, lying in the directions  $\theta$  and equidistant from the array, the resultant values of electric field intensity plotted as radii, with the corresponding values of  $\theta$  as angle, give a polar pattern which is the directional diagram of the array.

The values of the phase angles  $\phi$  may be computed from the parameters of the array, but are more readily determined graphically. If the array is drawn to scale, unit length on the drawing being equal to one wave length, the lengths of the path differences  $\delta$  will be equal to the phase angles  $\phi$  expressed as a fraction of a complete revolution; that is, of  $360^\circ$ . Thus, if a unit length (that is, one wave length to the scale of the drawing of the array) is divided into 360 equal parts, each part equivalent to  $1^\circ$ , and the lengths of the path differences laid off on this scale, the angular values of  $\phi$  may be read directly in degrees.

It has been found convenient to combine this ( $\delta, \phi$ ) conversion scale with a protractor which is also fitted with a circular scale for the inclusion of  $\alpha$ . Three ( $\delta, \phi$ ) conversion scales are provided, corresponding to scales of 4, 8, and 12 inches, respectively, equal to one wave length in the scale drawing of the array. They occupy the lower

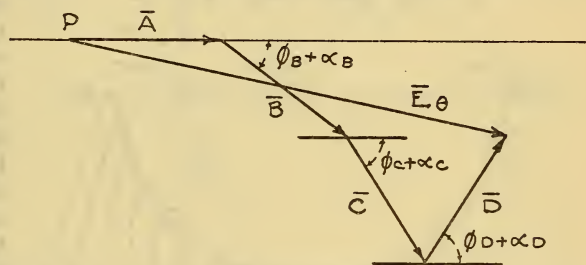


FIGURE 2.—Vector diagram giving the resultant electric field intensity at  $P$  due to the four sources of Figure 1



half while the time phase or  $\alpha$ -scale occupies the upper half of the protractor as shown in Figure 3.

As an example of the use of the protractor, let it be required to find the angle  $(\phi_B + \alpha_B)$  between **B** and **A** of Figure 2, where these vectors represent the effects at *P* of the elements *B* and *A*, respectively of Figure 1. Assume the current in *B* to be leading that in *A* by one-eighth period; that is,  $\alpha = +T/8$ . The center of the protractor is placed at the head of the reference vector **A** and the instrument rotated in a counter-clockwise direction until the action line of *A* (in this case its tail, extended if necessary) coincides with  $T/8$  on the positive  $\alpha$ -scale. With the instrument in this position, the length of  $\delta_B$ , taken from Figure 1 (drawn to scale 4 inches =  $\lambda$ ) with dividers, is laid off on the 4-inch scale from the origin for negative  $\delta$ . The correspond-

ing angle  $\phi$  marks a point on the action line of the required vector **B** which is directed through the center of the protractor toward the  $\phi$ -scale.

If  $\alpha$  had been negative the protractor with its center at the head of **A** would have been rotated in a clockwise direction until  $T/8$  on the negative  $\alpha$ -scale coincided with the action line of **A** (in this case the head of **A**, extended if necessary). With the instrument in this position a  $\delta$  would have been laid off as before or in case  $\delta_B$  had been positive, its length would have been laid off from the origin for  $+\delta$ . The

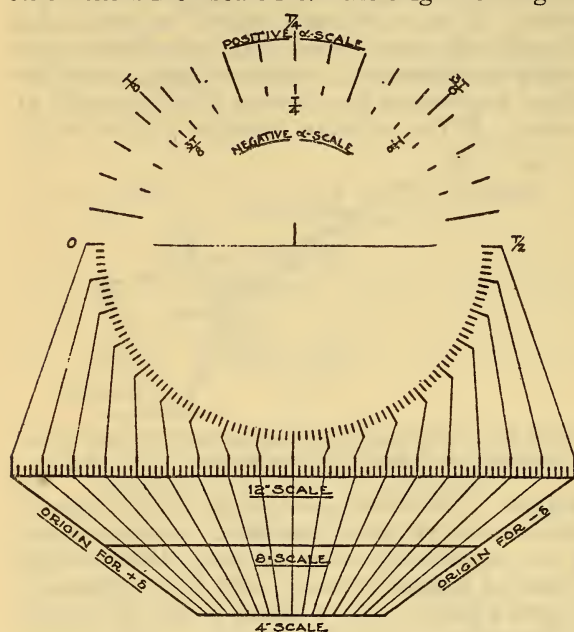


FIGURE 3.—Special protractor for conveniently determining and combining the time phase angles  $\alpha$  and the space phase angles  $\phi$  in vector diagram

corresponding angle  $\phi$  in this case would determine a point on the action line of the required vector **B** directed from the  $\phi$ -scale through the center of the protractor.

When path differences greater than  $\frac{\pi}{2}$  occur, the following procedure is used: As many half-wave lengths as possible are measured along the path difference and the protractor (after it has been set for the proper time phase angle  $\alpha$ ) is rotated through  $180^\circ$  for each one-half wave length so measured. The remainder of the path difference (which is less than one-half wave length) is laid off on  $\delta$ -scale as previously described.

## III. APPLICATIONS OF METHOD

As illustrations of the method, the steps in plotting polar diagrams of two very simple arrays will be outlined here. The first array (shown in fig. 4) consists of two antennæ separated by a distance equal to one-half wave length and carrying equal equiphased currents. This is the simplest type of broadside array. The direction  $\theta = 0^\circ$  is perpendicular to the line joining the antennæ, and the antenna  $A$  is considered as the reference standard. This array has two axes of symmetry ( $\theta = 0$  and  $\theta = 90^\circ$ ) so that it is necessary to determine the polar pattern for one quadrant only, the others being exactly similar.

A convenient method of determining the path differences  $\delta_B$  for points  $P$  lying in different directions from the array is illustrated in Figures 4 and 5. It is evident from Figure 4 that the angle  $BMA$  is a right angle and that as  $P$  moves from the direction  $\theta = 0^\circ$  to  $\theta = 90^\circ$  the locus of  $M$  is a semicircle which circumscribes the right triangle  $BMA$  and has  $AB$  for its diameter. This construction is shown in Figure 5, where  $AB$  is drawn equal to one-half wave length to the scale chosen, and  $BM_{10}$ ,  $BM_{20}$  are the required path differences when  $P$  lies in the directions  $\theta = 10^\circ$ ,  $\theta = 20^\circ$ , etc.

A length must now be chosen for the vector  $A$  which represents the electric field intensity at  $P$  due to the antenna  $A$ . Since there are two antennas with equal equiphased currents, the maximum possible field intensity is twice that due to  $A$  alone, so that the length used for  $A$  must be half of the maximum length of radius desired on the polar diagram. For diagrams of simple arrays, 4 inches is a convenient maximum; then  $A$  may be made 2 inches long. This length is laid off on a reference line, as in Figure 6, and the phase angles  $\phi$  measured from its end, the values of  $\phi$  being obtained from Figure 5 and converted to  $\phi$ 's by means of the protractor described. From the termination of  $A$ , vectors  $B$  of the same length as  $A$  are drawn, each corresponding to the proper phase angle  $\phi_s$ . The vector sums  $A + B$ , represented by the heavy lines in Figure 6, are the magnitudes of the radii of the directional diagram, so that these lengths from the vector diagram may be transferred directly to polar coordinate paper by means of dividers to give the polar pattern of the array. This is shown in Figure 7.

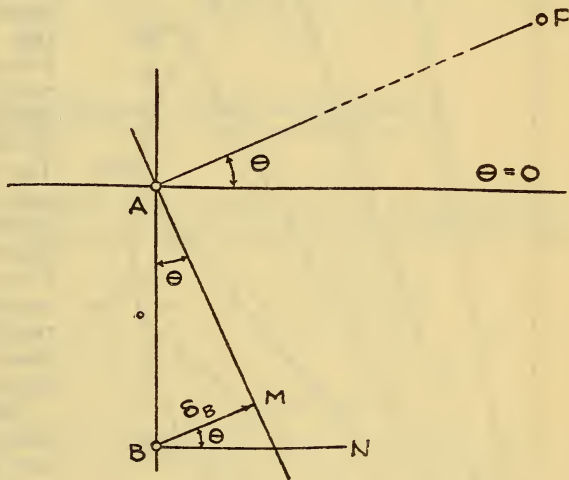


FIGURE 4.—Arrangement of two equiphased antennæ with  $\lambda/2$  spacing

Another very simple array is the end-on array of two antennas in Figure 8. Here the antennas are separated by one-fourth wave length, and the currents in them are equal but in phase quadrature, the current in *B* leading that in *A*. The direction  $\theta=0$  lies in a line joining the two antennas, and the antenna *A* is again taken as reference. This array has but one axis of symmetry ( $\theta=0$ ), so that radiation in the directions  $\theta=0^\circ$  to  $180^\circ$  must be determined.

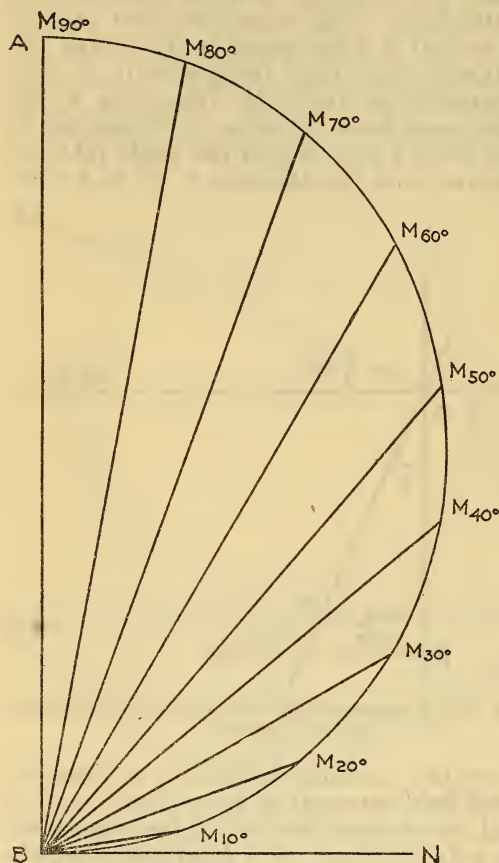


FIGURE 5.—Section *ABN* of Figure 4 drawn to scale

The lengths  $AM_\theta$  are the retardations in the directions  $\theta$  from the array

As before, the values of  $\delta$  are the lengths, between *B* and points *M* lying on a semicircle of diameter *AB*. Values of  $\delta$ , as *P* moves in  $10^\circ$  steps through the first quadrant are shown in Figure 9. As *P* moves through the second quadrant  $\delta$  changes sign but duplicates the  $\delta$ -lengths of the first quadrant. All the required path differences may, therefore, be obtained from Figure 9. The vector diagrams for this case, drawn by means of the protractor are shown superimposed one on the other in Figure 10, where, to avoid confusion, only a few of the resultants are drawn. The resulting polar pattern is shown in Figure 11.

Figure 12 illustrates a principle which is very useful in the determination of polar patterns of arrays having a large number of elements. Let *E* represent the field intensity at *P* due to the group of elements *AB*, in which *A* has been taken as reference for the group, and let *E'* represent the field intensity of a similar group *A'B'* in which *A'* has been taken as reference, then the vector sum  $\mathbf{E} + \mathbf{E}'$  represents the effects at *P* of both groups. The angle between *E* and *E'* will be the sum of the time phase angle between the currents in *A* and *A'* and the space phase angle corresponding to the path difference  $\delta'$ .

If the group *A'B'* is not exactly similar to the group *AB*, account must be taken of the relative differences of phase of *E* and *E'* in different directions since, as may be seen from Figures 6 and 10, the angle between the vector resultants of these two dissimilar groups in the direction  $\theta=10^\circ$  is not the same as the angle between them in the



direction  $\theta = 20^\circ$ . These differences must be included in determining the phase angles between the vectors  $\mathbf{E}$  and  $\mathbf{E}'$  and are obtained from the vector diagrams for the two groups.

This method for adding the effects of groups of antennas is particularly valuable in determining the directional characteristics of

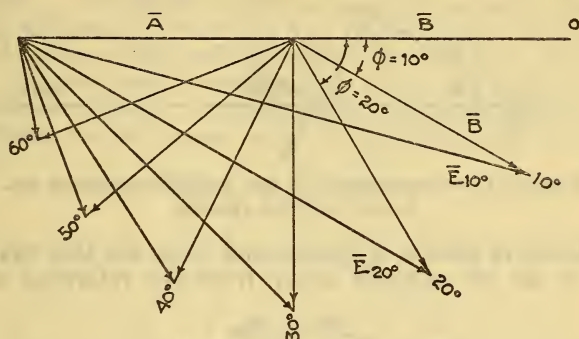


FIGURE 6.—Vector diagrams showing how the effects of antennas  $A$  and  $B$  of Figures 4 and 5 are added at the points  $P_\theta$

linear arrays of large numbers of antennas, and in calculating the effects of the ground. In the case of a linear array, the resultant due

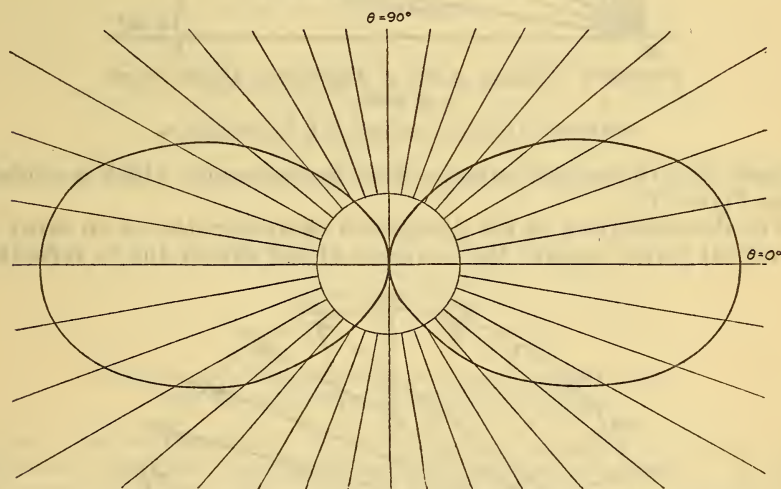


FIGURE 7.—Polar pattern of an array consisting of two equiphased elements with  $\lambda/2$  spacing

to two antennas at one end of the array is first computed. Let the phase angle between these two components be  $\phi_1$ , the resultant being denoted by  $\mathbf{E}_1$ . Then the effect due to the first four antennas may be obtained by adding to  $\mathbf{E}_1$  another vector of equal length, the angle between the two being  $2\phi_1$ . This resultant is added to another of

equal length and an angle of  $4\phi_1$  to give the resultant for the first eight antennas, and so on. This procedure follows from the method

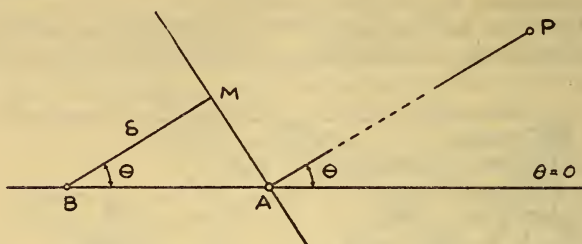


FIGURE 8.—Arrangement of two quadrature-phased antennas with  $\lambda/4$  spacing

for the addition of effects of groups and from the fact that the path difference of the  $n^{\text{th}}$  antenna away from the reference is equal to

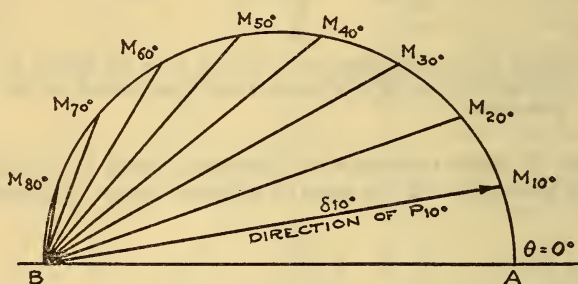


FIGURE 9.—Section ABM of Figure 8 is shown drawn to scale

The lengths  $AM_i$  are the radiations  $\delta_i$  in the directions  $P_i$ .

$n$  times that of the first antenna from the reference, which is evident from Figure 12.

The determination of the directional characteristics of an array in a vertical plane requires the inclusion of the effects due to reflection

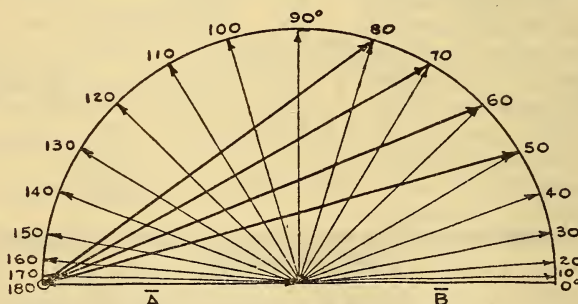


FIGURE 10.—Vector diagrams showing how the effects of antennas A and B of Figures 8 and 9 are added at the points  $P_i$

Only four of the resultants are shown.

from the earth. In this case, the polar pattern of the array is first determined neglecting the ground effects. Then the effects due to the image are added to those due to the array itself by the method

already described, the construction being indicated in Figure 13. It will be noted that the field intensity in a direction  $\theta$  is determined by the addition, with proper phase angle, of the intensity due to the array in the direction  $\theta$  and the intensity in the direction  $-\theta$ , the magnitude of the latter being multiplied by the reflection coefficient of the ground. The phase angle must include not only the angle due to the path difference  $\delta'$ , but also any phase change at reflection and the relative phase difference between the effects in the directions  $\theta$  and  $-\theta$ . If the array is symmetrical about the line  $\theta=0$ , this last phase difference is zero. In calculating the magnitudes and phases of the currents in the image array, the ground may be considered

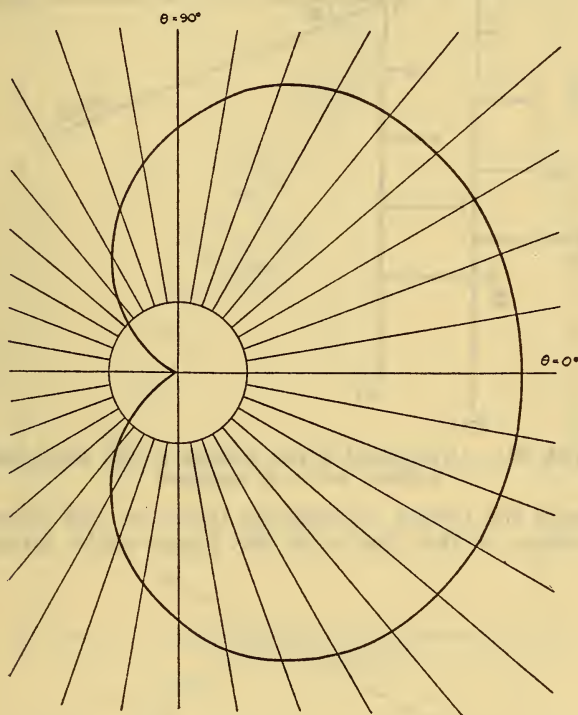


FIGURE 11.—Polar pattern of an array consisting of two quadrature-phased elements with  $\lambda/4$  spacing

(1) as a perfect conductor, (2) as a perfect insulator, or (3) as an imperfect conductor, depending on the surrounding terrain. In the last case, equations and curves given by Wilmotte<sup>8</sup> are very convenient and have been applied here. The angle designated as  $\theta$  by Wilmotte is the angle  $A\hat{b}c$  of Figure 13. In most cases it may be considered equal to the complement of the angle  $\theta$  of that figure.

To facilitate the determination of the vectors representing the image antenna effect, the multiplication chart shown in Figure 14 was made. It is an adaptation of the  $Z$ -type nomographic or align-

<sup>8</sup> R. M. Wilmotte, General Formulae for the Radiation Distribution of Antenna Systems, J. I. E. E., vol. 68, p. 1174, September, 1930.



ment chart. The length of vector due to the array is laid off from  $A$  on the antenna scale and from the terminus of this vector, a line is

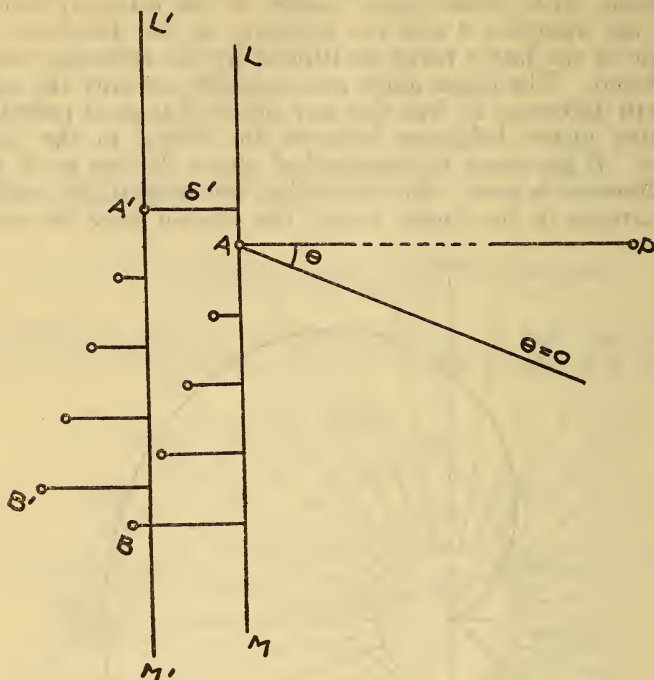


FIGURE 12.—Arrangement of two antenna groups whose polar patterns are to be combined

drawn through the proper multiplying factor on the diagonal scale. The intersection of this line with the image scale determines the

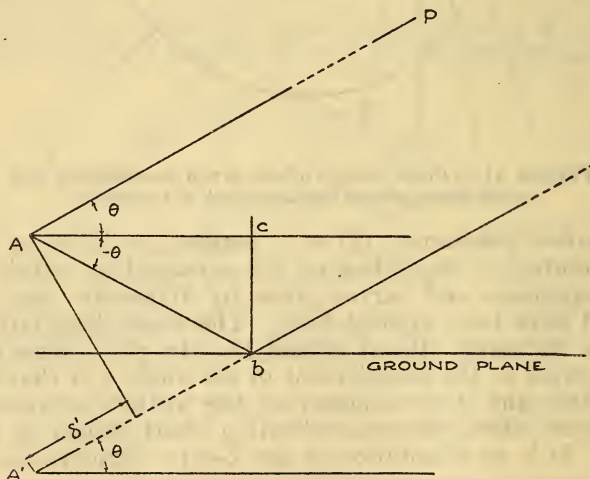


FIGURE 13.—Construction for determining the effect of antenna image

magnitude of the required vector. Practically, these multiplications can be carried out very rapidly with a divider and straightedge.

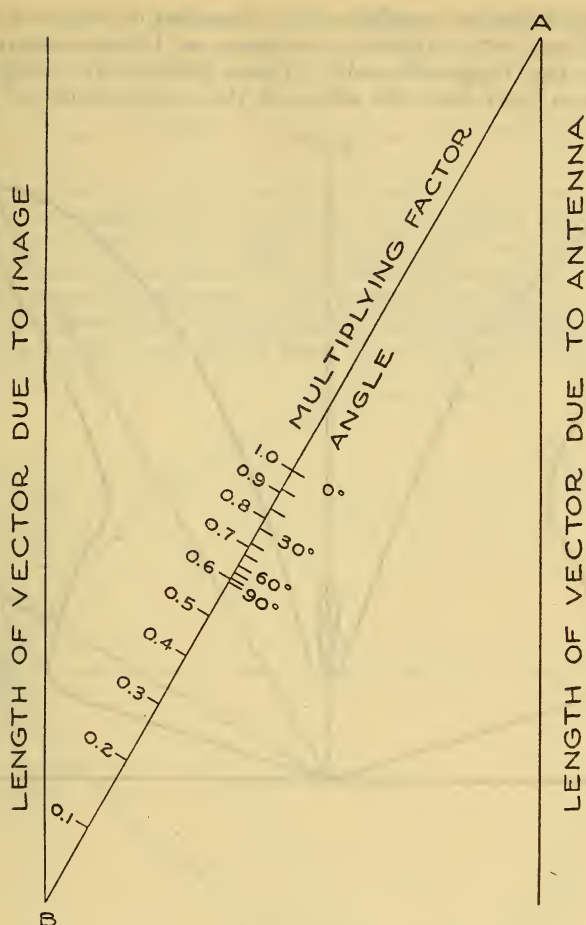


FIGURE 14.—Multiplying chart for determining the effect of antenna image

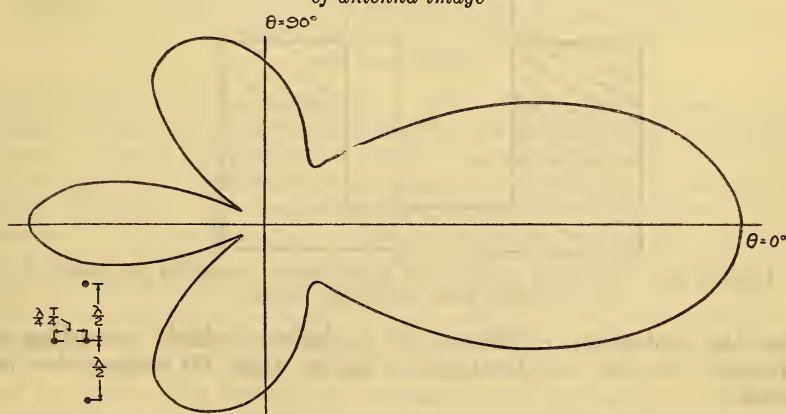


FIGURE 15.—Polar pattern of four elements with phasing and spacing as indicated

Effect of image is neglected

Values of the reflection coefficient for a number of values of  $\theta$  between  $0^\circ$  and  $90^\circ$  and for a dielectric constant of 15 were computed and marked on the diagonal scale. These points are valid only for frequencies so high that the effect of the conductivity of the earth

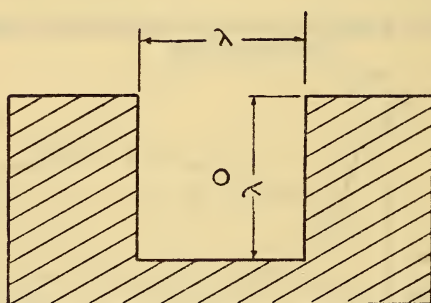
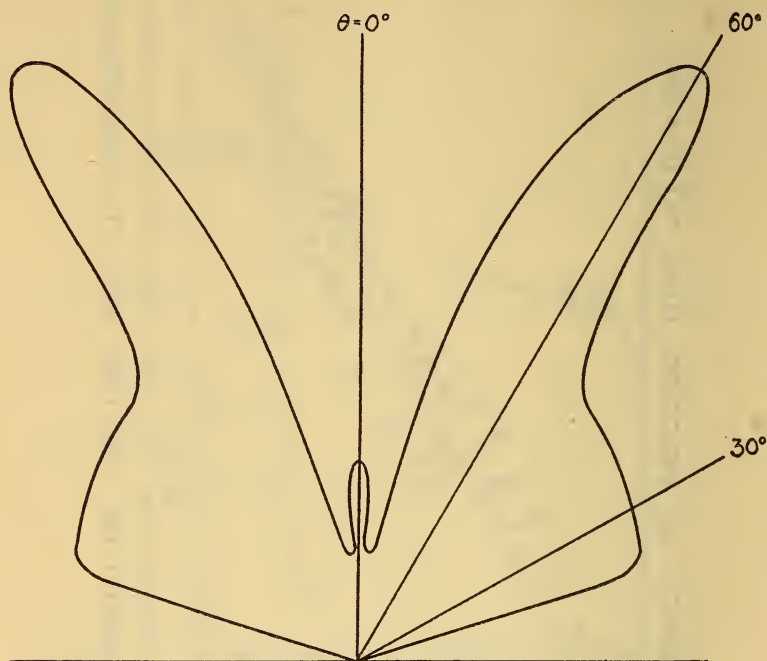


FIGURE 16.—The polar pattern of a single source located at the center of a trough in an insulating medium

upon the reflection coefficient is negligible, which according to Wilmotte,<sup>9</sup> is true for frequencies higher than 60 megacycles per second.

<sup>9</sup> See footnote 8, p. 563.



Figures 15 and 16 illustrate polar patterns obtained by methods described. The directive pattern of Figure 15 can be checked analytically from its equation, which in polar coordinates is

$$r = \sqrt{[1 + 2 \cos(\pi \sin \theta)]^2 + 2 [1 + 2 \cos(\pi \sin \theta)] \sin \left( \frac{\pi}{2} \cos \theta \right) + 1}$$

Figure 16 shows the radiation from a single source located at the center of cross section of a trough in an insulating medium. The width and the depth of the trough are each equal to one wave length.

Figures 17 and 18 illustrate the magnitude and nature of the effects of the earth in some instances. The first of these figures is the polar pattern in free space for an end-on array of eight antennas spaced one-fourth wave length and with a time phase difference of one-fourth

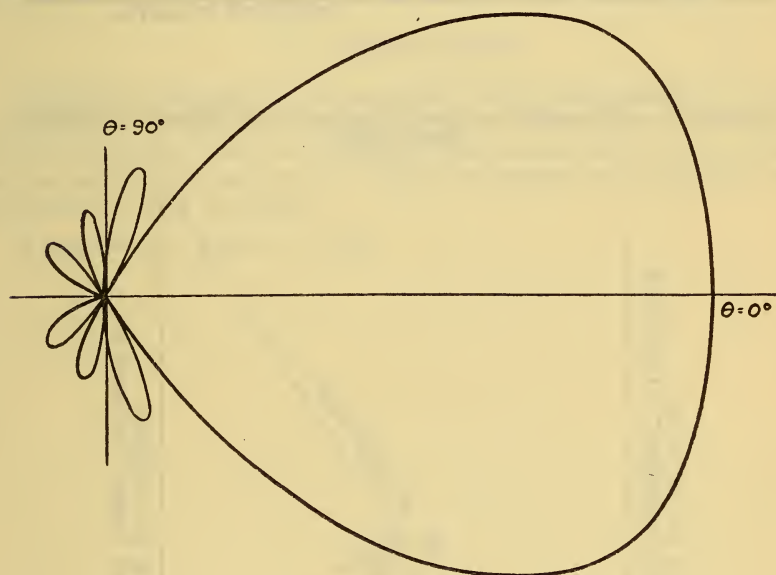


FIGURE 17.—Polar pattern of an end-on array of 8 elements with  $\lambda/4$  spacing and quarter-period phasing

Image effects neglected.

period between adjacent antennas. This type of array is very closely similar to that selected by Dunmore<sup>10</sup> for a landing beam for aircraft. Figure 18 shows the pattern of the same array placed one wave length above ground. Wilmotte's equations were used to determine the image currents. The available observations on the radiation characteristics of the actual array indicate that the calculated pattern is very nearly correct. The differences may readily be attributed to differences between the actual and theoretical arrays, and to the fact that the actual array is slightly tilted, while the calculated diagram is based upon a horizontal array. It is evident that the major portion of the directive efficiency is due to the broadside effect of the array and its image, the horizontal extension serving merely to eliminate unwanted lobes. This is of course also evident from equations derived

<sup>10</sup> H. Diamond and F. W. Dunmore, A Radiobeacon and Receiving System for Blind Landing of Aircraft, B. S. Jour. Research, vol. 5 (R.P238), p. 897, October, 1930.

by Wilmotte<sup>11</sup> which show that maximum directivity is obtained when the array is extended in a direction perpendicular to the desired

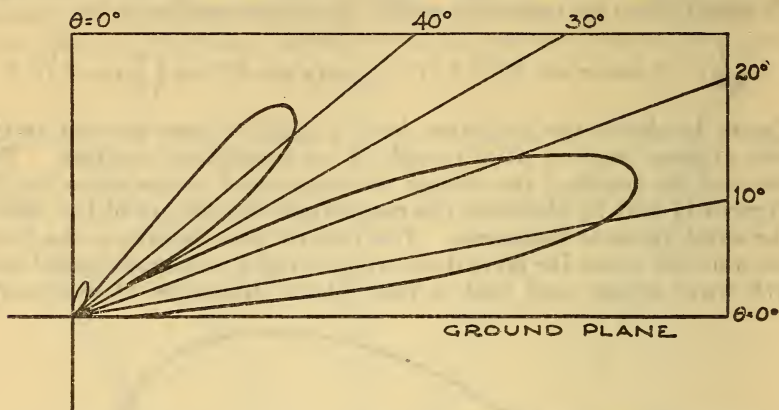


FIGURE 18.—Polar pattern of same array as that of Figure 17, including effect of image

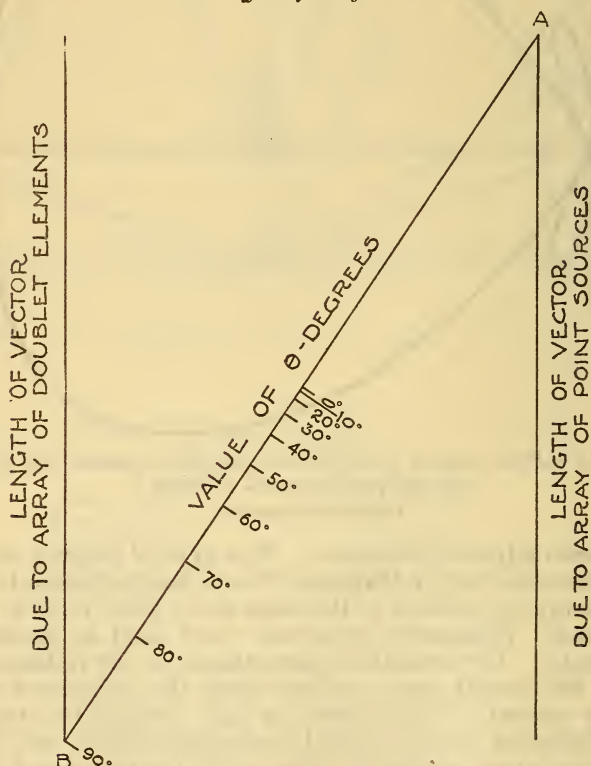


FIGURE 19.—Multiplying chart for modifying the polar pattern of an array of point sources to include the directivity of doublet elements

direction of maximum radiation. It will be noted also that the angle of elevation of the beam is dependent primarily upon the height of

<sup>11</sup> R. M. Wilmotte, General Considerations of the Directivity of Beam System. J. I. E. E., vol. 66, p. 955, September, 1928.

the array above ground, the effects of slight variations of the array from the horizontal being of the second order.

When the individual elements of the array have an inherent directivity of their own, the polar pattern of the array obtained by considering the elements as point sources must be modified to include this inherent directivity. Thus if the polar pattern in the containing plane of an array of half-wave antennæ is desired it is necessary to multiply each radius of the point source pattern by  $\cos \theta$ . This may be readily done by means of the *Z*-type chart shown in Figure 19, which is used in exactly the same way as the chart of Figure 14. The length of vector representing  $E$  at  $P_\theta$ , from the point source array, is laid off from  $A$  on the right-hand vertical scale of the chart. Then the corresponding value of  $E'$  at  $P_\theta$ , from the array of half-wave elements is obtained from the left-hand vertical scale.

#### IV. CONCLUSION

Graphical methods are well adapted to the determination of polar patterns of directional antenna systems. The labor involved is considerably less than that required for mathematical computation and is further reduced by the special protractor and graphical multiplication charts described.

WASHINGTON, March 9, 1932.







